

Dynamic behaviour of cement mortars reinforced with glass and basalt fibres

Luigi Fenu^{1*}, Assistant Professor

¹University of Cagliari, Department of Civil Engineering, Environment Engineering, and Architecture,
Via Marengo 2, 09123 Cagliari, Italy

Daniele Forni², Assistant Professor

²University of Applied Sciences of Southern Switzerland, DynaMat Lab, 6952 Canobbio, Switzerland

Ezio Cadoni², Professor

²University of Applied Sciences of Southern Switzerland, DynaMat Lab, 6952 Canobbio, Switzerland

Abstract

In this paper, the dynamic behaviour of cement mortars reinforced with both glass and basalt fibres is studied. The influence of the addition of both types of fibre on energy absorption and tensile strength at high strain-rate was investigated, and the performance of the two types of fibre-reinforced mortar was compared. For this aim, basalt and glass fibres with same diameter and length were used. Static tests in compression, in tension and in bending were first performed. Dynamic tests by means of a Modified Hopkinson Bar were then carried out in order to investigate how glass and basalt fibres affected energy absorption and tensile strength of the fibre reinforced mortar at high strain-rate. The Dynamic Increase Factor (DIF) was finally evaluated. The experimental results show that DIF is not significantly affected by the addition of basalt and glass fibres, while energy absorption at high strain rate is significantly increased by the addition of glass fibres and only slightly increased by the addition of basalt fibres.

Keywords:

A. Glass fibres; B. Impact behaviour; B. Fracture toughness

*Corresponding author. Tel.: +39 070 6755386; fax: +39 070 6755403

E-mail address: lfenu@unica.it

Elsevier: "© . This manuscript version is made available under the CC-BY-NC-ND 4.0 license <https://creativecommons.org/licenses/by-nc-nd/4.0/>
DOI: <https://doi.org/10.1016/j.compositesb.2016.02.035>
Article published in: Composites Part B: Engineering
Volume 92, 1 May 2016, Pages 142-150

1. Introduction

Even if the use of glass fibres to reinforce concrete was first proposed in Russia before the 2-nd World War, the industrial use of Glass Fibre Reinforced Concrete (GFRC) dates back to the 1970's, after the development by Pilkington Corporation in 1967 of a suitable formulation to produce Alkali-Resistant glass fibres containing zirconia [1].

Nowadays glass fibres with improved alkali resistance allow a structural use of GFRC [2-3], otherwise limited by the embrittlement of glass fibres caused by the alkaline environment of the Portland cement paste.

Therefore, GFRC was extensively used in the industrial production of prefabricated elements, especially precast façade panels.

While many articles describe the static behaviour of GFRC, its dynamic behaviour has been much less studied. A reference study on toughness and impact tests on GFRC panels was carried out by Mobasher and Shah [4].

Glinicki et al [5] studied impact on GFRC plate specimens through the drop weight instrumented test device that allowed to detect the maximum impact load, the energy absorbed up to the maximum load, and the energy absorbed up to total failure, thus obtaining an impact-to-static energy absorption ratio falling within the range 1.7–1.8 for the GFRC plate elements considered.

The impact behaviour of facade panels made of GFRC was investigated by Enfedaque et al. [6] by shooting steel spheres with high velocity on square samples of different GFRC panels, and by then calculating energy absorption as the kinetic energy difference of the projectile before and after impact.

Yldirim et al. [7] studied the impact behaviour of different Fibre Reinforced Concretes (FRC) including GFRC. Using practically the same drop-weight method of ACI 544 2R-89 [8], impact tests were performed time after time on cubical FRC samples with side 100 mm until failure occurred. Glass fibres were shown to be as effective as steel fibres and more effective than polypropylene fibres to prevent first cracking. Samples reinforced with steel fibres needed a much higher number of impact tests until failure occurred with respect to samples reinforced with glass and polypropylene fibres, that both needed almost the same number of impacts to reach failure. Adding glass fibres to steel fibres was very effective to delay failure, better than adding polypropylene fibres.

Sangeetha [9] studied the favourable effect of additives such as superplasticizer, air retaining agent and retarder on impact strength of GFRC plates.

Comparison of the characteristics of glass and basalt fibres has been done in few articles. Wei et al. [10] studied their differences in terms of environmental resistance and mechanical performance, finding that basalt fibres are in general suitable for being used in both acid and alkali environments, but acid resistance of glass fibres is much less than that of basalt fibres.

Basalt fibres are suitably used to reinforce concrete panels and domes. Monolithic domes made of concrete reinforced with basalt fibres have been successfully built using a technology developed by the Monolithic Dome Institut [11]. The use of basalt fibres is suitable in concrete structures subjected to fire (i.e. to reinforce concrete segments for tunnelling) because of the high melt-point of basalt (see Table 1). In fact, a common use of basalt fibres is in the fire protection sector. Ipbüker et al. [12] studied cement–basalt mixtures for their radiation shielding properties, finding that basalt fibre has good potential as an addition to heavyweight concrete because, while improving its mechanical properties in terms of strength and toughness, does not reduce shielding against gamma and neutron radiation for long-term applications in nuclear energy industry.

Concrete beams and panels, as well as industrial and road pavements reinforced with basalt rebar have been recently realized [13]. Since it does not rust, is particularly suitable for environments where corrosion is a continuous concern. Moreover, it is 89% percent lighter than steel, that is an important feature for developing its use in civil engineering: for instance, one man can easily lift a 150 m coil of basalt rebar 10 mm in diameter.

Static behaviour of Basalt Fibre Reinforced Concrete (BFRC) is less known than that of GFRC. A reference study was carried out by Felicetti et al. [14]. Sim et al. [15] and Jiang et al. [16] investigated basalt fibre as a strengthening material for concrete structures and observed that, besides increasing tensile strength and toughness of concrete, have good resistance to chemical attack, even if Sim et al. [14] observed that also basalt fibres are sensitive to alkali attack, although less sensitive than glass fibres. Also, Kabay [17] studied the use of basalt fibres in increasing tensile strength and fracture energy of concrete, together with resistance to abrasion, also finding that the addition of basalt fibres resulted in reduction in the compressive strength. Tehmina Ayub et al. [18] studied the use of basalt fibres together with silica fume or met kaolin in preparing High Performance Fibre Reinforced Concrete HPFRC. Santarelli et al. [19] proposed lime-based mortars reinforced with basalt fibres as a possible bio-based material for ancient masonry restoration.

While noting that not only glass but also basalt fibres are sensible to alkali attack, Lipatov et al. [20] studied basalt fibres produced with appropriate zirconia content (using $ZrSiO_4$ as a zirconium source) to improve

their resistance to alkali attack, thus improving also in the long-term the mechanical properties of BFRC through highly reducing fibre corrosion in the cementitious matrix.

Moreover, very few articles on the dynamic behaviour of BFRC can be mentioned. Lai and Sun [21] studied the dynamic behaviour of Ultra-High Performance Cementitious Composites (UHPCC) reinforced by only steel fibres and by hybrid fibres, the latter consisting of basalt fibres or polyvinyl alcohol (PVA) fibres added to steel fibres. The addition of basalt fibres showed to be effective on improving impact strength of UHPCC, but less effective than the addition of the same percentage of PVA fibres.

Strain-rate behaviour of a basalt fibre reinforced mortar was investigated by Asprone et al. [22] by means of dynamic tests at medium ($0.5\div 3.0\text{ s}^{-1}$) and high strain rate ($50\div 90\text{ s}^{-1}$) carried out, respectively, through a Hydro-Pneumatic Machine and a Modified Tensile Hopkinson Bar device. Fracture energy obtained from dynamic tests was shown to be higher than that obtained from quasi-static tests, and the Dynamic Increase Factor (DIF) for tensile strength was shown to be increased by increasing values of strain rate.

Lai et al. [23] showed that resistance to repeated penetration and different depth explosion in Ultra High Performance Concrete (UHPC) is improved significantly by hybrid reinforcement of steel and basalt fibres.

In this paper the different performances under dynamic loading of mortars reinforced with glass and basalt fibres were compared. The dynamic behaviour in tension of both types of fibre reinforced mortar was investigated. Dynamic tensile tests at high strain rate were performed by means of a Modified Tensile Hopkinson Bar device. Since the specimen diameter was 20 mm (depending on the size of the heads of the Modified Tensile Hopkinson Bar device), fine aggregates were used, thus suggesting to carry out the experimental study on mortar specimens and not on concrete specimens.

Also, reference static tests to evaluate flexural, compressive, and tensile strength (the latter to be compared with dynamic tensile strength through the Dynamic Increase Factor) were carried out on both types of mortar. To allow to compare the performance in reinforcing mortar of the two types of fibre, specimens reinforced with straight glass and basalt fibres were prepared using fibres with same size (in both diameter and length) and same fibre content (in weight).

Not straight fibres (for instance spiral) could be more effective in dissipating impact energy and in increasing tensile strength, especially under dynamic loading conditions at high strain rates [24]. Unfortunately, it is impossible to achieve not straight glass and basalt fibres with same shape, so that their performance comparison would be affected by their different shape. Hence, for this reason, in this study straight glass and basalt fibres with same diameter and length were chosen.

2. Experimental procedure

2.1 Materials and specimen preparation

Both types of specimen (reinforced with glass and basalt fibres) were prepared using Standard Portland cement (CEM I, 52.5 R as prescribed by EN 197-1 [25]) and standard sand, in accordance with EN 196-1 [25]. From this cementitious mixture, a reference cement mortar without fibres (binder to aggregate ratio = 0.5, water over cement ratio $w/c = 0.5$, cement content 635 kg/m^3 , sand content 1270 kg/m^3) was first prepared. The fibre reinforced specimens were then prepared by adding a given fibre content (in weight) of glass and basalt fibres to the cementitious mixture. The water/cement ratio of 0.5 was kept constant for all the investigated compositions.

To better compare the respective performance in reinforcing concrete under dynamic loading conditions, glass and basalt fibres with same size (12 mm in length and $14 \mu\text{m}$ in diameter) were chosen. For the same reason, both types of specimen were prepared with same fibre content (3% and 5% in weight). Four different types of fibre reinforced mortar were hence obtained. Alkali-resistant glass fibres with high zirconia content were used. Mechanical and physical properties of both glass and basalt fibres are those provided by their manufacturer, and are reported in Table 1.

After mixing, the cementitious mixtures were poured into the steel mould to manufacture prismatic specimens ($40 \times 40 \times 160 \text{ mm}^3$), whose surfaces were made plane and covered by means of a polyethylene film. Water evaporation during the first hours was thus avoided, and all the specimens were then cured at a temperature of 20°C and a relative humidity (RH) of 95% for 28 days before testing.

Prismatic specimens ($40 \times 40 \times 160 \text{ mm}^3$) were used for static flexural and compression tests, while specimens for dynamic tests were obtained by coring cylindrical specimens (diameter $d=20 \text{ mm}$, height $L=20 \text{ mm}$) from the prismatic ones. Apparent density of specimens with 3 and 5% glass and basalt fibres was determined, and the same average value of, respectively, 2.155 and 2.156 g/cm^3 was obtained. Apparent density, as expected, was practically unaffected by the slight difference of specific gravity between glass and basalt fibres (see Table 1).

2.2 Experimental tests

Flexural strength f_r and compressive strength f_c under static loading were first evaluated on both the reference mortar and on the samples reinforced with 3 and 5% of glass and basalt fibres. Four specimens for

each mortar type were prepared. Taking into account that f_r is strictly correlated to the tensile stress of the fibre reinforced mortar and is however much lower than f_c (even if f_r resulted increased and f_c decreased by fibre addition), f_r was evaluated in accordance with EN 196-1 [26] by means of the three-point bending test (with $f_r = 1.5PL/h^3$, P = applied force at mid-length of the prismatic specimen, L = distance between its end supports, h = side of its square section). The compressive strength f_c was then evaluated carrying out the compression test on the two prism halves obtained from the bending test.

Dynamic tests were performed by means of a Modified Hopkinson Bar (MHB) device (see Figure 1), placed in the DynaMat Laboratory of the University of Applied Sciences of Southern Switzerland (SUPSI), Lugano, Switzerland.

Figure 1. The Modified Tensile Hopkinson Bar device used in this experimental research

The MHB device consisted of two circular aluminium bars, called input and output bars, both 20 mm in diameter but with different lengths of 3 m and 6 m, respectively. The sample was glued between these bars using a bi-component epoxy resin. The input bar was connected to a high strength steel pretension bar (6 m in length and 12 mm in diameter), that was used as pulse generator. The way of performing the test and a deep description of the MHB device used in this research is widely reported in [27-28].

The Hopkinson bar device is considered as a profitable technique in order to characterise the material behaviour at high strain rate, as proofed by a large amount of papers published in this field [27-31].

To this aim, an incident pulse ε_I propagates along the input bar without modifying its length and diameter. After reaching the specimen, a reflected pulse ε_R is hence generated by the specimen as a part of the incident pulse, whereas the other part, the transmitted pulse ε_T , passes through the specimen and propagates into the output bar.

Thereafter, the stress, the strain and the strain-rate in the sample can be, respectively, derived from the following equations:

$$\sigma_E(t) = E_0 \frac{A_0}{A} \varepsilon_T(t) \quad (1)$$

$$\varepsilon_E(t) = - \frac{2C_0}{L} \int_0^t \varepsilon_R(t) dt \quad (2)$$

$$\dot{\varepsilon}(t) = -\frac{2C_0}{L}\varepsilon_R(t) \quad (3)$$

where, L is the specimen length, A_0 is the cross-sectional area of output and input bars, A is the initial cross-sectional area of the specimen gauge length portion, E_0 is the elastic modulus of the bars, $C_0 = (E_0/\rho)/2$ is the bar elastic wave speed, ρ is the bar density and t is time.

3. Results

The values of static flexural and compressive strength are summarised in Table 2. It shows that, under static conditions, flexural strength was significantly increased by the addition of glass fibres and even more by basalt fibres.

The increase of tensile strength means that the bond developed between fibres and mortar was effective under static conditions, since otherwise no increase of tensile strength due to fibre addition would have been possible [32]. Compressive strength of the reference mortar was instead significantly higher than that of the samples reinforced with both glass and basalt fibres, meaning that the fibre reinforced samples behaved as if fibres were inclusions scattered throughout the mortar. This is frequent in fibre reinforced cementitious materials [33-34] because, unless the fibre content is very low (lower than about 1% [33]), the fibres in the mix are not as effective as aggregates (for same volume) to resist compressions. It is herein confirmed by the fact that the higher was the content of both glass and basalt fibres, the lower was the compressive strength of the mortar.

Dynamic tests at high strain-rate were then carried out by means of the MHB device. The consequent stress-rate ranged between 500 and 600 GPa/s. In order to achieve accurate stress-strain diagrams at high strain-rate, stresses and displacements were detected at high frequency (1 Msample/s), thus allowing to calculate energy absorption and get the maximum stress with good precision.

Through carrying out tensile tests at high strain-rate on both the reference mortar and on mortars reinforced with glass and basalt fibres, the influence of the addition of both types of fibre on energy absorption and tensile strength of samples subjected to high impact loading was investigated.

Tables 3-7 report the experimental results for each test carried out on mortar samples reinforced with the two types of fibre, as well as on the reference mortar. In particular, the *Stress-Rate* is the slope of the stress flow evaluated as a function of time in the elastic regime, *Max Tensile Stress* is the highest value obtained for

each test, while *Fracture strain*, *Fracture time* and *Displacement at fracture* are the corresponding strain, time and displacement values respectively. *Failure time* is the time value when the stress goes back to zero after failure. Eventually, *Total energy* is the energy represented by the area under the stress-crack opening displacement curve.

Figure 2 allows to compare the dynamic behaviour of the mortar reinforced with 3% and 5% of glass (Figure 2a) and basalt (Figure 2b) fibres with that of the reference mortar.

Figure 2. Stress in function of displacement for reference mortar, and glass (a) and basalt (b) reinforced mortars.

The addition of both types of fibre, affected the post-peak behaviour under dynamic conditions, especially when glass fibres were used.

It can be observed that the addition of 3% and even more of 5% of glass fibres (samples G3% and G5%) significantly improved the post- peak behaviour, with energy absorption at high strain rate much higher than in the reference mortar (Fig.2a). The improved post-peak behaviour under dynamic conditions is also highlighted by the much higher failure time of both G3 and G5 mortars (Tables 4 and 5) with respect to that of the reference mortar. The addition of 3% basalt fibres (samples B3%) slightly improved the post peak behaviour of the fibre reinforced mortar, giving it only slightly higher toughness with respect to the reference mortar. Nevertheless, both total energy and failure time were almost the same of the reference mortar (Table 6). The addition of 5% of basalt fibres (samples B5%) was instead more effective in increasing energy absorption, thus giving the mortar slightly higher toughness (Table 7). Total energy of samples B5% was almost one third higher than that of samples B3%. Nevertheless, its total energy was shown to be about one fourth of that of samples G5%, and its failure time was only slightly increased with respect to that of the reference mortar.

Compared to basalt fibres, glass fibres were hence more effective in increasing dynamic energy absorption at high strain rate (Fig.2b), considered by some authors [35] as mainly due to debonding between fibres and the cementitious matrix. Fibre debonding occurred in specimens reinforced with both types of fibre (see Figure 3) but, since fibres with same geometry were used (that is with same length, diameter and shape), and the mix of both types of fibre reinforced specimen was also the same (same aggregates, water and cement type, same cement content as well as same binder on aggregate ratio, same w/c ratio, same fibre content, same preparation procedure including curing), the higher energy absorption of specimens reinforced with glass fibres is likely due to the different chemico-physics properties of the surface of the two types of

fibres.

Figure 3. Images obtained through multifocal microscopy (magnification 200x) of the failure sections of samples reinforced with 3% basalt (a) and glass (b) fibres. Debonded fibres are well evident.

Figure 4 shows the images obtained through Scanning Electron Microscopy (SEM, 2500x magnification) of both types of fibre debonded during a dynamic tensile test at high strain rate. It can be seen that debonding modified the fibre surface, that was shown to be much smoother in new fibres (before use) than how it was after debonding from the cementitious matrix (Compare Figures 4a and 4b with Figures 4c and 4d). Moreover, it can be seen that the surface of glass and basalt fibres after debonding was different. In fact, the surface of glass fibres resulted almost completely covered by a thin surface layer formed by the products of reaction between the outer alkali resistant glass of the fibre and the cementitious matrix, while the surface of basalt fibres resulted damaged and only partially covered by the products of reaction between the basalt fibre and the cementitious matrix. Therefore, under dynamic loading, debonding of glass fibres involved a thin layer of reaction products covering almost the whole fibre surface and protecting the intact inner part of the glass fibre.

Figure 4. Images obtained through Scanning Electron Microscopy (SEM, 2500x magnification) of new basalt (a) and glass (b) fibres before being used, and of debonded basalt (c) and glass (d) fibres.

Conversely, only a part of basalt fibre was shown to be covered by the thin layer of reaction products, while a significant part of this thin surface layer resulted peeled after debonding. This means that impact loading was able to remove the outer thin layer of reaction products formed on the surface of the basalt fibre, because corrosion due to alkali attack altered both surface properties of the basalt fibre and its bond with the cementitious matrix. Debonding of damaged fibres was therefore shown to not dissipate energy, thus reducing energy absorption under dynamic loading of specimens reinforced with basalt fibres.

Nevertheless, the influence of the chemico-physics properties of the surface of fibres made of different materials on bond with a cementitious matrix should be investigated in particular with a specific study.

Figure 5 allows to easier compare the values (reported in Tables 3-7) of total energy of both types of reinforced mortar and of the reference one. It clearly shows that the addition of glass fibres significantly increased total energy under impact loading, that was instead almost unaffected by the addition of basalt fibres, even if the post-peak behaviour was influenced by their addition (see Fig.2b). Figure 5 also shows that the standard deviation values of the results of the tests on specimens reinforced with 3 and 5% glass

fibres is higher than those of specimens reinforced with same content of basalt fibres. Unfortunately this mainly depends on the fact that the number of tested specimens reinforced with both 3 and 5% glass fibres was only three (while for basalt fibres was four), because, for both sets of four specimens prepared with 3 and 5% glass fibres, one specimen of each set was damaged while performing the test. Nevertheless, the better effectiveness of glass fibres in improving energy absorption under dynamic conditions at high strain rate is very well evident.

Figure 5. Comparison of total energy for different fibre contents in both glass and basalt reinforced mortars.

Figure 3 shows the images obtained through multifocal microscopy (magnification 200x) of the failure sections of samples reinforced with 3% of basalt and glass fibres, where both types of debonded fibres under dynamic conditions are well evident.

No macroporosity was observed. As far as it regards microporosity, considered as sum of gel porosity and capillary porosity, only the latter can affect strength of the cementitious mortar depending on water/cement ratio and hydration of the cement paste [36], that for specimens reinforced with both types of fibres were however the same, because all were prepared with same water/cement ratio, and all were mixed and cured with the same procedure and for the same time. This fact, together with the fact that the apparent density of the different fibre reinforced mortars (all with fibres with same geometry) only slightly varied when changing the fibre content and not when changing the fibre type, should confirm that the higher dynamic energy absorption of specimens reinforced with glass fibres with respect to those reinforced with basalt fibres would depend on the different surface properties of the two types of fibres.

Finally, a comparison of Tables 4, 5, 6 and 7 with Table 3 shows that contrary to static tensile strength, dynamic tensile strength was only slightly increased by fibre addition, because fibre debonding did not allow tensile strength to be significantly increased.

Also, the Dynamic Increase Factor (DIF) was evaluated (Figure 6) as the ratio between the dynamic strength and the static strength of the material. For this aim, by using the same specimen geometry used for high strain-rate tensile tests, also direct static tension tests (0.5 MPa/s) were performed, according to UNI 6135 [37]. Testing three specimens for each mortar RM, G3%, G5%, B3%, B5%, their tensile strength resulted, respectively, 5.11 ± 0.0 , 5.23 ± 0.5 , 5.24 ± 1.2 , 6.10 ± 0.9 , 5.97 ± 0.7 MPa.

Figure 6. Dynamic Increase Factor vs. Stress-rate.

For the reference mortar, DIF 2.30 was obtained, that is a typical expected value for this material. The lowest

fibre addition (3%) led to a DIF slight increase for only mortar G3% (2.44), while mortar B3% (2.29) was shown to have almost the same DIF value of the reference mortar. Fibre addition until 5% brought on DIF values of 2.29 and 2.14 for mortars G5% and B5%, respectively, thus lower than the DIF values of both G3% and B3% mortars.

Hence, DIF was shown to be little affected by fibre addition, and to vary little with fibre content. It can be also noted a low DIF decrease with the fibre content increase of both glass and basalt fibres from 3% to 5%. This means that, under dynamic conditions, the increase of fibre content was ineffective to improve micro-crack bridging.

Therefore, as seen before, comparison with plain mortars shows that the addition of fibres (especially of glass fibres), while improving energy absorption under dynamic loading, practically does not affect tensile strength.

Compared to the other fibre-reinforced concrete, glass fibre-reinforced concrete is a highly competitive material in applications such as permanent formworks, pipes, refurbishment of buildings, sewer liners, tunnel cladding, façade panels. This is due to its excellent mechanical properties, fire resistance, easy moldability and high corrosion resistance. Also basalt fibre-reinforced concrete is in general suitable for these applications, but is instead much less used.

By improving toughness, glass and basalt fibres can be suitably used in the above applications also to protect from impact (i.e. façade panels subjected to collisions). Moreover, in applications where impact and exceptional actions at high strain rate (like blasts and collisions) are possible to occur, a protective (often sacrificial) layer made of glass (or basalt) fibre-reinforced mortar can be provided in order to absorb a part of impact energy.

4. Conclusions

In this article the performance of basalt and glass fibres in reinforcing a cementitious mortar subjected to impact loading at high strain rate is compared. For this aim, same content of straight glass and basalt fibres with same size in diameter and length were used. and the fibre-reinforced specimens were tested by using a Modified Hopkinson Bar (MHB) device at high strain-rate (with a consequent stress rate of 500 - 600 GPa/s). From these dynamic tensile tests, the following conclusions have been gathered:

- while static flexural strength of the mortar was significantly increased by the addition of both glass and basalt fibres, dynamic tensile strength resulted practically unincreased (only slightly) by the addition of both types of fibre

- the addition of both glass and basalt fibres to the cementitious mortar improved its post-peak behaviour under dynamic tension loading.
- total energy resulted highly increased by the addition of 5% glass fibres (7.2 times the fracture energy of the reference mortar), but was significantly increased also by a fibre content of 3% (4.6 times that of the reference mortar).
- even if the addition of 5% basalt fibres improved the post-peak behaviour of the mortar, fracture energy was only slightly increased (2.2 times the fracture energy of the reference mortar); the post-peak behaviour was improved also by the addition of 3% basalt fibres, but total energy resulted practically unchanged with respect to the reference mortar, owing to the higher maximum stress of the latter.
- DIF of mortars reinforced with both glass and basalt fibres was practically the same as that of the reference mortar.

Therefore, for straight fibres with same diameter and length, basalt fibre reinforcement was shown to be less performing than glass fibre reinforcement when used under dynamic conditions at high strain rate.

This research is a first contribution to study the comparison of the dynamic behaviour of mortars reinforced with different mineral fibres. Further research is needed, in particular it would be interesting to investigate the effect of different fibre shapes and of the chemico-physics properties of the fibre surface on bond with the cementitious matrix.

Acknowledgements

The contribution and funding of the Dynamat Laboratory of SUPSI University, Canobbio (Switzerland), is acknowledged.

This article is also a fruit of the scientific collaboration between the Dynamat Laboratory of SUPSI University and the Faculty of Engineering and Architecture of the University of Cagliari, started with Prof. Ezio Cadoni's visit at the University of Cagliari as Visiting Professor in the years 2007 and 2010 and funded by the Autonomous Region of Sardinia (Italy).

References

1. J.P.J.G. Ferreira and F.A.B. Branco, The Use of Glass Fiber-Reinforced Concrete as a Structural Material, *Exp Techniques* 2007; 31(3):64-73.

2. Cian D, Della Bella B. Structural Applications of GRC for Precast Floors. In: Proceedings of the 12th Int. GRCA Congress, Dublin Camberley (UK), October, 2001. p.41–52.
3. Branco F, Ferreira J, Brito J, Santos J. Building Structures with GRC. In: Proceedings of CIB World Building Congress, Wellington (NZ), April, 2001. p.1-11.
4. Mobasher B, Shah SP. Test parameters for evaluating toughness of Glass Fiber Reinforced Concrete. *ACI Mat. J.*, 1989; 86:448–58.
5. Glinicki MA, Vautrin A, Soukatchoff P, Francois-Brazier J. Plate impact testing method for GRC materials. *Cem Concr Compos* 1994; 16(4):241-51.
6. Enfedaque A, Cendón D, Gálvez F, Sánchez-Gálvez V. Failure and impact behaviour of facade panels made of glass fibre reinforced cement (GRC). *Eng Fail Anal* 2011; 18(7):1621-1908.
7. Taner Yildirim S, Cevdet E. Ekinci, Fehim Findik. Properties of Hybrid Fiber Reinforced Concrete under Repeated Impact Loads. *Russ J Nondestruct+* 2012; 46(7):538-546.
8. ACI 544 2R-89. Measurement of properties of fiber reinforced concrete. American Concrete Institute 1989, Reapproved 1999.
9. Sangeetha P. Study on the compression and impact strength of GFRC with combination of admixtures. *J Eng Res & Stud* 2011; 2(2):36-40.
10. Wei B, Cao H, Song S. Environmental resistance and mechanical performance of basalt and glass fibers. *Mat Sc Eng A–Struct* 2010; 527:4708–15.
11. <http://www.monolithic.org/>
12. Ipbüker C, Nulk H, Gulik V, Biland A, Tkaczyk AH. Radiation shielding properties of a novel cement–basalt mixture for nuclear energy applications. *Nucl Eng Des* 2015; 284, 27-37.

13. Ramakrishnan V, Tolmare NS., Brik VB. Performance Evaluation of 3-D Basalt Fiber Reinforced Concrete & Basalt Rod Reinforced Concrete. Final Report for Highway IDEA (Innovation Deserving Exploratory Analysis programs) Project 45. Transportation Research Boards of the National Accademies, November 1998).
14. Felicetti R, Meyer C, Shimanovich S. Basalt fiber reinforced oil well cement slurries. In: Proceedings of the 3-rd Int. Conference on Concrete under Severe Conditions. Vancouver, June, 2001. p.18-20.
15. Sim J, Park C, Do Young Moon. Characteristics of basalt fiber as a strengthening material for concrete structures. *Comp: Eng Part B* 2005; 36 (6–7), 504–512.
16. Jiang C, Fan K, Wu F, Chen D. Experimental study on the mechanical properties and microstructure of chopped basalt fibre reinforced concrete. *Mater Design* 2014; 58, 187–193
17. Kabay N. Abrasion resistance and fracture energy of concretes with basalt fiber. *Constr Build Mat* 2014; 50, 95-101.
18. Ayub T, Shafiq N, Nuruddin MF. Mechanical Properties of High- Performance Concrete Reinforced with Basalt Fibers. *Procedia Eng* 2014; 77, 131–139.
19. Santarelli ML, Sbardella F, Zuena M, Tirillò J, Sarasini F. Basalt fiber reinforced natural hydraulic lime mortars: A potential bio-based material. *Mater Design* 2014; 63, 398-406
20. Lipatov YV, Gutnikov SI, Manylov MS, Zhukovskaya ES, Lazoryak BI. High alkali-resistant basalt fiber for reinforcing concrete. *Mater Design* 2015;73, 60-66.
21. Lai JZ, Sun W. Dynamic damage and stress-strain relations of Ultra-High Performance Cementitious Composites subjected to repeated impact. *Science China, Technological Sciences* 2010; 53(6):1520–1525.

22. Asprone D, Cadoni E, Iucolano F, Prota A. Analysis of the strain-rate behaviour of a basalt fiber reinforced natural hydraulic mortar. *Appl Mech & Mat.* 2011; 82:196-201.
23. Lai J, Guo X, Zhu Y. Repeated penetration and different depth explosion of ultra-high performance concrete. *Int J Imp Eng* 2015; 84:1-12.
24. Xu Z, Hao H, Li HN. Mesoscale modelling of dynamic tensile behaviour of fibre reinforced concrete with spiral fibres. *Cem Concr Res* 2012; 42:1475-1493.
25. EN 197-1. Cement – Part 1: Composition, specifications and conformity criteria for common cements. European Committee for Standardization 2011.
26. EN 196-1. Methods of testing cement – Part 1: Determination of strength. European Committee for Standardization 2005
27. Cadoni, E. Dynamic Characterization of Orthogneiss Rock Subjected to Intermediate and High Strain Rates in Tension, *Rock Mech Rock Eng* 2010; 43:667-676.
28. Cadoni E, Fenu L, Forni D. Strain rate behaviour in tension of austenitic stainless steel used for reinforcing bars. *Constr Build Mat* 2012; 35:399-407.
29. Cadoni E, Meda A, Plizzari GA. Tensile behaviour of FRC under high strain-rate. *Mater Struct* 2009; 42:1283-1294.
30. Caverzan A, Cadoni E, di Prisco M. Tensile behaviour of high performance fibre-reinforced cementitious composites at high strain rates. *Int J Impact Eng* 2012; 45:28-38.
31. Erzar B, Forquin P. An experimental method to determine the tensile strength of concrete at high rates of strain. *Exper Mech* 2010, 50(7); 941-955.
32. Karihaloo BL. *Fracture mechanics & Structural concrete.* Longman Group Limited, 1995.

33. Malagavelli V, Rao PN. Effect of non bio degradable waste fibres in concrete slabs, *Int J Civ & Str Eng*, 2010,1(3):449-457.
34. Kruszka L, Moćko W, Cadoni E, Fenu L. Comparative experimental study of dynamic compressive strength of mortar with glass and basalt fibres. In: *Proceedings of the 11-th International DYMAT Conference*, September 7-11, 2015, Lugano , Switzerland.
35. Caverzan A, Cadoni E, Di Prisco M. Dynamic tensile behaviour of high performance fibre reinforced cementitious composites after high temperature exposure, *Mech Mat*, 2013, 59(4):87-109.
36. Collepardi M. *The New Concrete*. Tintoretto, 2010.
37. UNI 6135. *Prove distruttive sui calcestruzzi. Prova di trazione*. Ente Nazionale Italiano di Unificazione, 1972 (in Italian).

TABLES

Table 1

Size, physical and mechanical properties of glass and basalt fibres as provided by the manufacturer.

| | Length [mm] | Diameter [μm] | Specific gravity [g/cm^3] | Softening point [$^{\circ}\text{C}$] | Tensile strength [N/mm^2] | Elastic modulus [kN/mm^2] |
|---------------|-------------|----------------------------|---|--|---|---|
| Glass fibres | 12 | 14 | 2.60 | 860 | 1000–1700 | 72 |
| Basalt fibres | 12 | 14 | 2.60–2.63 | 1050 | 3800–4000 | 89–93 |

Table 2

Flexural and compressive strength of reference and fibre reinforced mortars obtained through static tests.

| | Flexural strength [MPa] | Compressive strength [MPa] |
|------------------|-------------------------|----------------------------|
| Reference mortar | 6.57 ± 0.13 | 70.20 ± 1.65 |
| Glass fibre 3% | 7.78 ± 0.31 | 57.58 ± 2.44 |
| Glass fibre 5% | 8.37 ± 0.69 | 50.46 ± 2.13 |
| Basalt fibre 3% | 8.72 ± 0.97 | 57.15 ± 0.90 |
| Basalt fibre 5% | 8.53 ± 0.63 | 52.10 ± 1.42 |

Table 3

Results for the reference mortar.

| Sample | Stress rate [GPa/s] | Max tensile stress [MPa] | Fracture strain [%] | Fracture time [μ s] | Failure time [μ s] | Displ. at fracture [mm] | Failure displ. [mm] | Total energy [J/m ²] |
|----------------|---------------------|--------------------------|---------------------|--------------------------|-------------------------|-------------------------|---------------------|----------------------------------|
| RM_01 | 556 | 12.17 | 0.30 | 32 | 44 | 0.006 | 0.025 | 177.28 |
| RM_02 | 639 | 12.73 | 0.33 | 32 | 41 | 0.007 | 0.020 | 151.40 |
| RM_03 | 476 | 12.35 | 0.32 | 35 | 46 | 0.006 | 0.025 | 177.00 |
| RM_04 | 550 | 9.76 | 0.26 | 33 | 62 | 0.001 | 0.079 | 249.53 |
| Average | 555 | 11.75 | 0.30 | 33.0 | 48.25 | 0.005 | 0.037 | 188.80 |
| STD | 66 | 1.35 | 0.03 | 1.40 | 9.39 | 0.003 | 0.028 | 42.26 |

Table 4

Results for the mortar reinforced with glass fibres (3%).

| Sample | Stress rate [GPa/s] | Max tensile stress [MPa] | Fracture strain [%] | Fracture time [μ s] | Failure time [μ s] | Displ. at fracture [mm] | Failure displ. [mm] | Total energy [J/m ²] |
|----------------|---------------------|--------------------------|---------------------|--------------------------|-------------------------|-------------------------|---------------------|----------------------------------|
| G3%_01 | 412 | 10.77 | 0.35 | 34 | 218 | 0.007 | 0.681 | 815.19 |
| G3%_02 | 553 | 10.50 | 0.52 | 35 | 167 | 0.010 | 0.518 | 947.45 |
| G3%_03 | 496 | 15.05 | 0.33 | 36 | 272 | 0.006 | 0.867 | 1259.64 |
| Average | 487 | 12.11 | 0.40 | 35 | 219.0 | 0.008 | 0.689 | 1007.43 |
| STD | 71 | 2.55 | 0.10 | 1.0 | 52.51 | 0.002 | 0.175 | 228.21 |

Table 5

Results for the mortar reinforced with glass fibres (5%).

| Sample | Stress rate [GPa/s] | Max tensile stress [MPa] | Fracture strain [%] | Fracture time [μ s] | Failure time [μ s] | Displ. at fracture [mm] | Failure displ. [mm] | Total energy [J/m ²] |
|----------------|---------------------|--------------------------|---------------------|--------------------------|-------------------------|-------------------------|---------------------|----------------------------------|
| G5%_01 | 470 | 15.45 | 0.58 | 35 | 222 | 0.012 | 0.686 | 1536.27 |
| G5%_02 | 480 | 12.91 | 0.41 | 28 | 237 | 0.008 | 0.778 | 1214.67 |
| G5%_03 | 566 | 11.58 | 0.34 | 32 | 241 | 0.007 | 0.760 | 909.28 |
| Average | 505 | 13.31 | 0.44 | 31.7 | 233.33 | 0.009 | 0.741 | 1220.07 |
| STD | 52 | 1.97 | 0.12 | 3.5 | 10.02 | 0.003 | 0.049 | 313.53 |

Table 6

Results for the mortar reinforced with basalt fibres (3%).

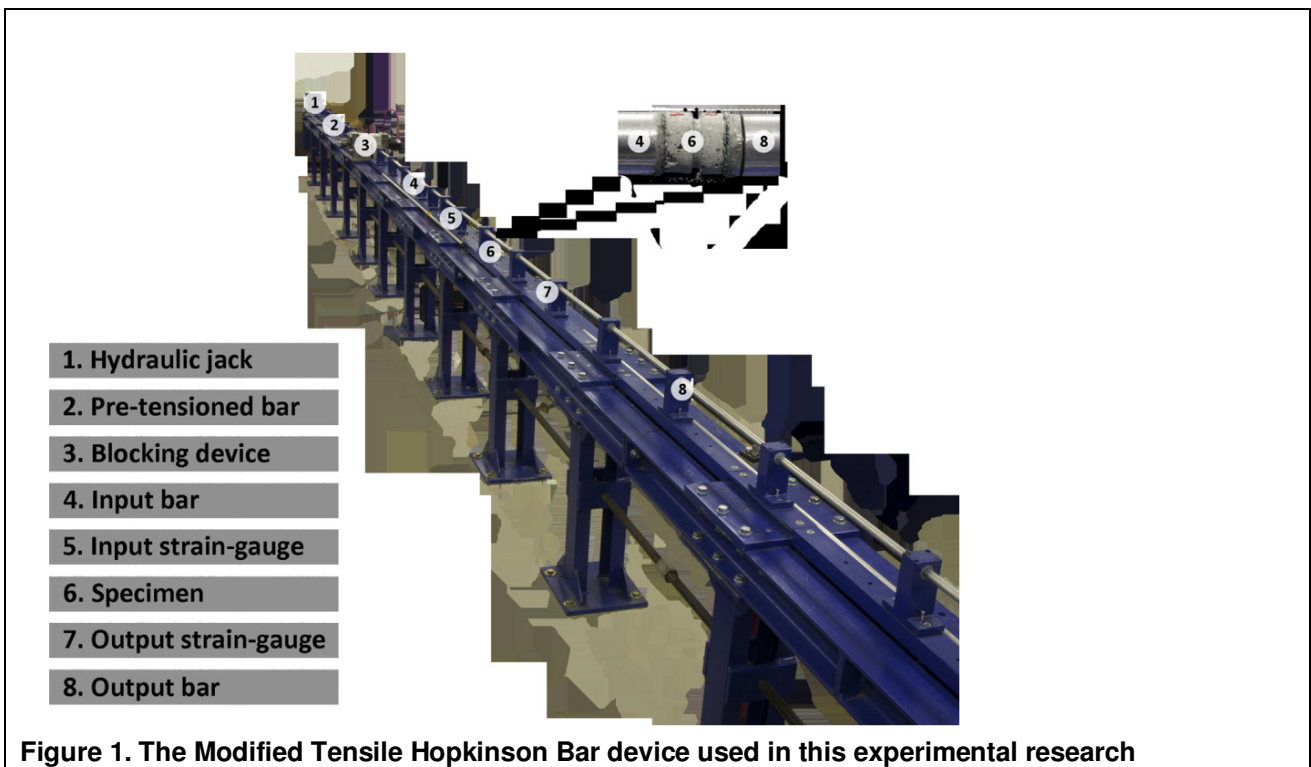
| Sample | Stress rate [GPa/s] | Max tensile stress [MPa] | Fracture strain [%] | Fracture time [μ s] | Failure time [μ s] | Displ. at fracture [mm] | Failure displ. [mm] | Total energy [J/m ²] |
|----------------|---------------------|--------------------------|---------------------|--------------------------|-------------------------|-------------------------|---------------------|----------------------------------|
| B3%_01 | 568 | 11.13 | 0.58 | 30 | 42 | 0.006 | 0.022 | 144.33 |
| B3%_02 | 691 | 12.97 | 0.35 | 30 | 41 | 0.007 | 0.023 | 173.98 |
| B3%_03 | 771 | 14.42 | 0.38 | 37 | 48 | 0.007 | 0.025 | 181.72 |
| B3%_04 | 256 | 17.43 | 0.22 | 39 | 65 | 0.005 | 0.065 | 260.99 |
| Average | 572 | 13.99 | 0.38 | 34.0 | 49.00 | 0.006 | 0.034 | 190.26 |
| STD | 226 | 2.66 | 0.15 | 4.7 | 11.11 | 0.001 | 0.021 | 49.83 |

Table 7

Results for the mortar reinforced with basalt fibres (5%).

| Sample | Stress rate [GPa/s] | Max tensile stress [MPa] | Fracture strain [%] | Fracture time [μ s] | Failure time [μ s] | Displ. at fracture [mm] | Failure displ. [mm] | Total energy [J/m ²] |
|----------------|---------------------|--------------------------|---------------------|--------------------------|-------------------------|-------------------------|---------------------|----------------------------------|
| B5%_01 | 748 | 13.65 | 0.34 | 36 | 54 | 0.007 | 0.040 | 216.88 |
| B5%_02 | 513 | 12.25 | 0.36 | 39 | 54 | 0.007 | 0.037 | 235.49 |
| B5%_03 | 456 | 12.29 | 0.41 | 34 | 46 | 0.008 | 0.028 | 185.78 |
| B5%_04 | 696 | 12.87 | 0.47 | 35 | 65 | 0.009 | 0.102 | 500.73 |
| Average | 603 | 12.76 | 0.39 | 36.0 | 54.75 | 0.008 | 0.052 | 284.72 |
| STD | 140 | 0.66 | 0.06 | 2.2 | 7.80 | 0.001 | 0.034 | 145.46 |

FIGURES



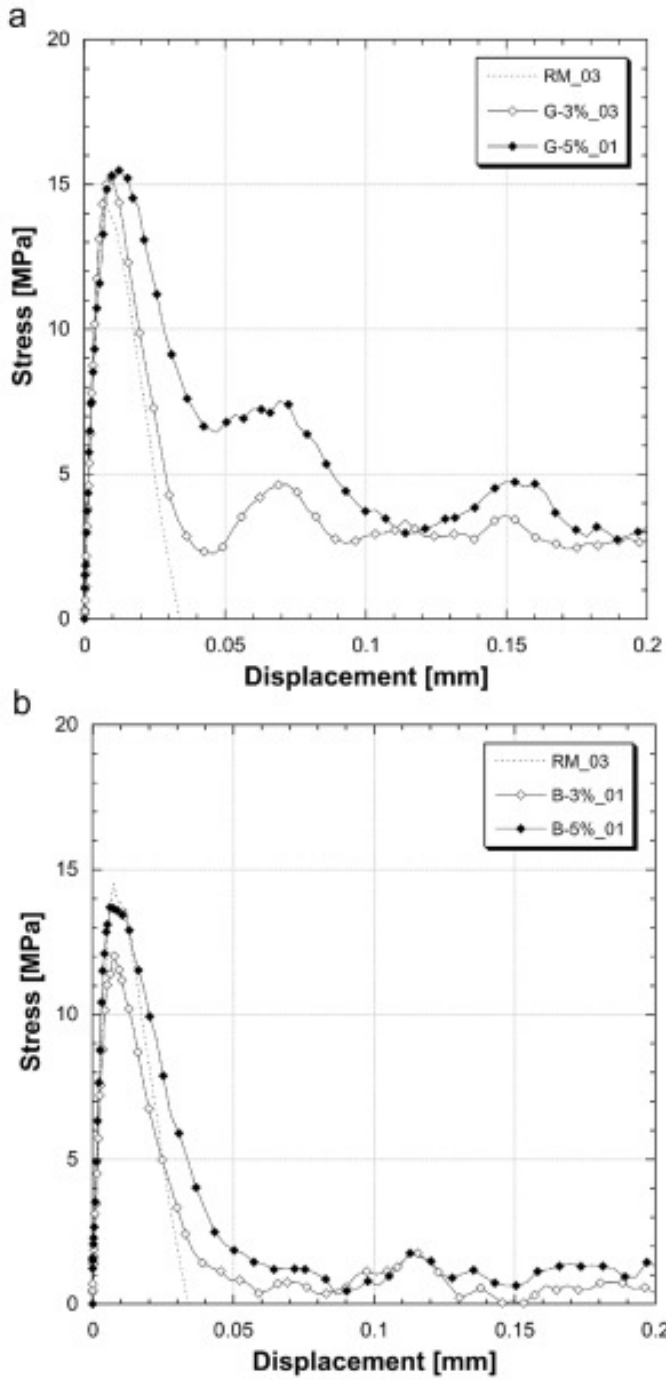


Figure 2. Stress in function of displacement for reference mortar, and glass (a) and basalt (b) reinforced mortars.

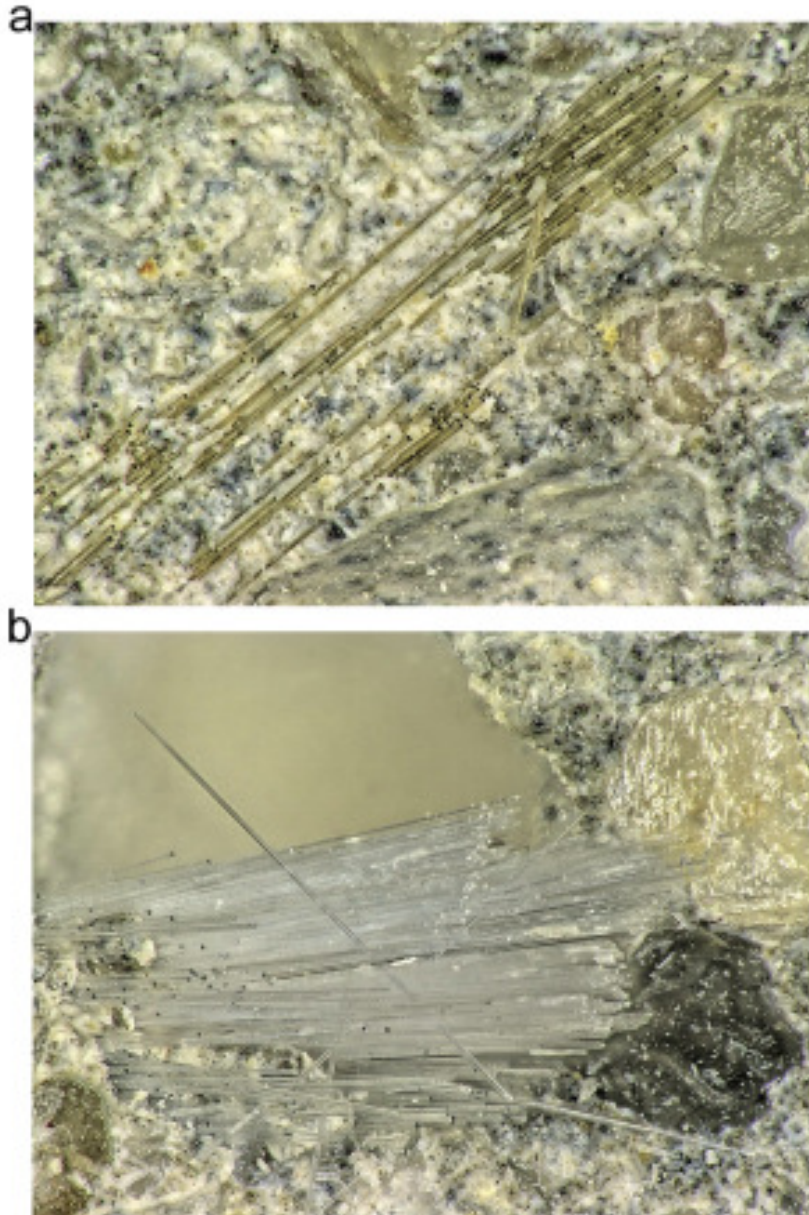


Figure 3. Images obtained through microfocal microscopy (magnification 200x) of the failure sections of samples reinforced with 3% basalt (a) and glass (b) fibres. Debonded fibres are well evident.

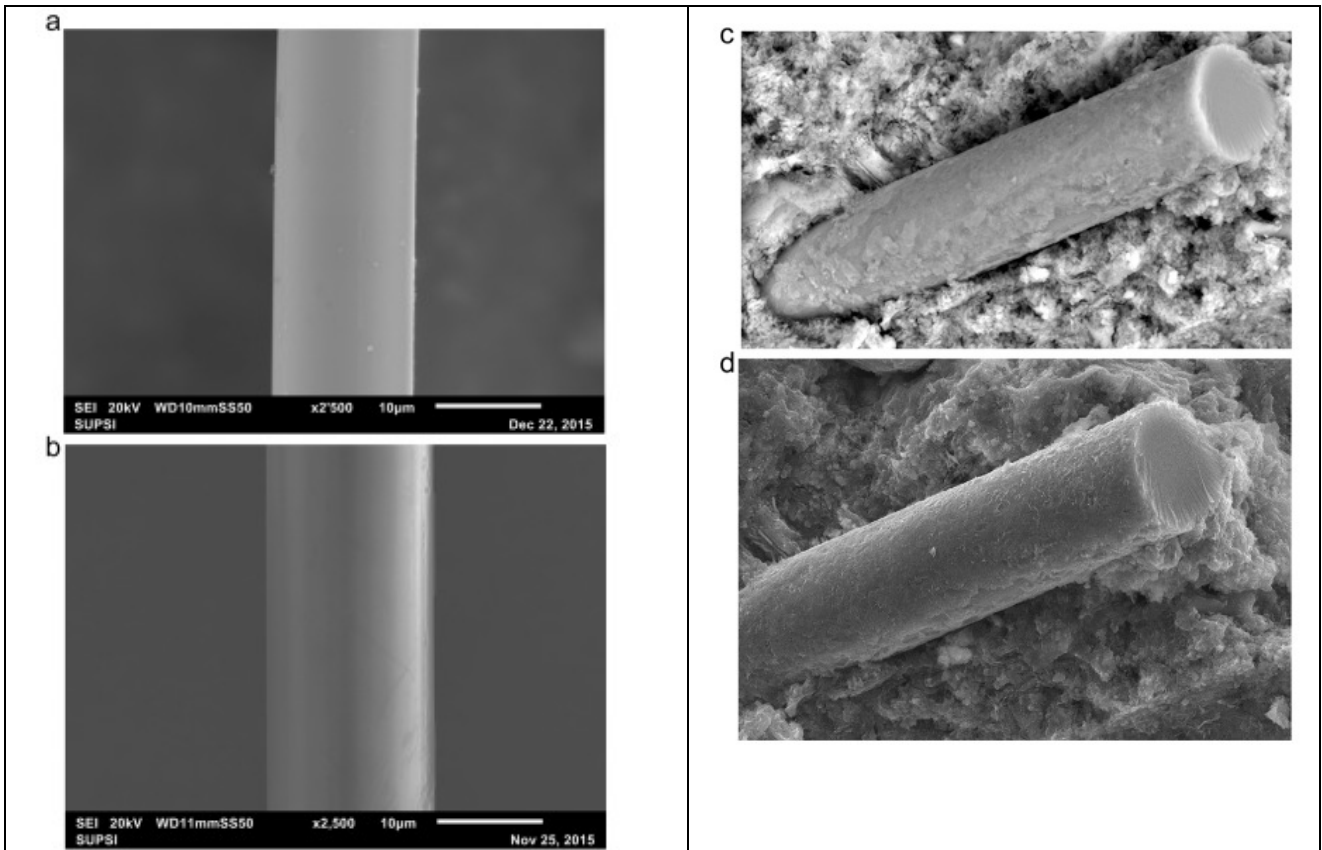


Figure 4. Images obtained through Scanning Electron Microscopy (SEM, 2500x magnification) of new basalt (a) and glass (b) fibres before being used, and of debonded basalt (c) and glass (d) fibres.

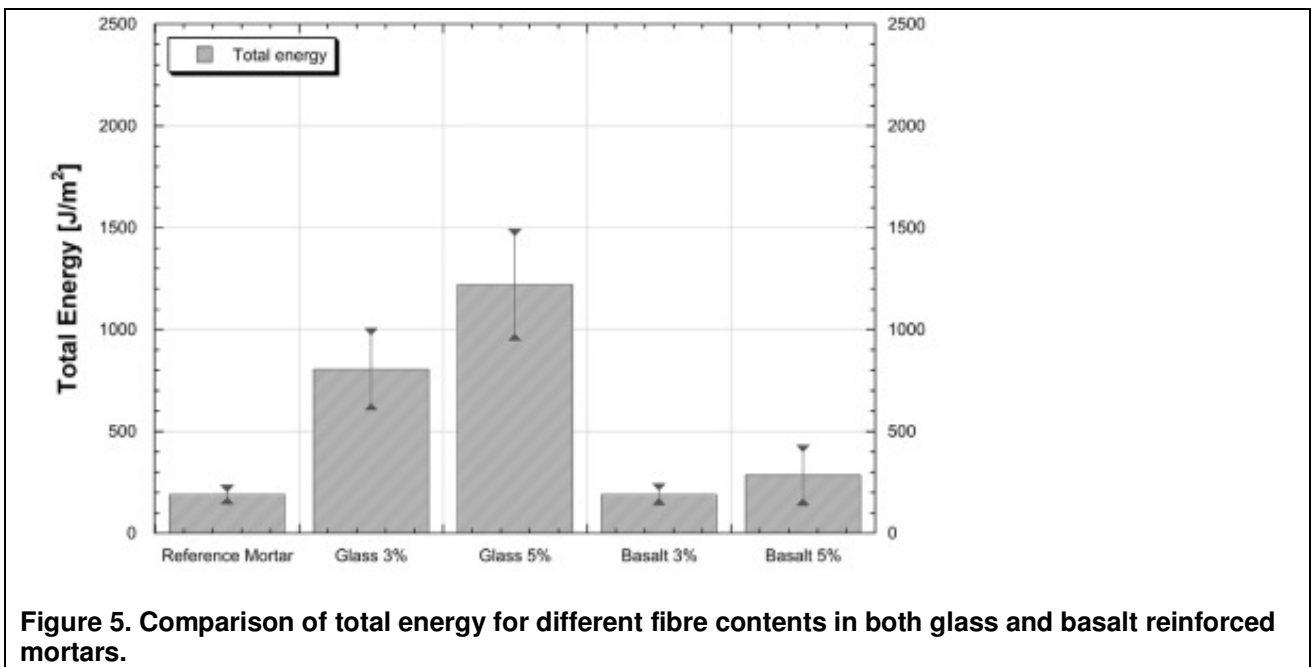


Figure 5. Comparison of total energy for different fibre contents in both glass and basalt reinforced mortars.

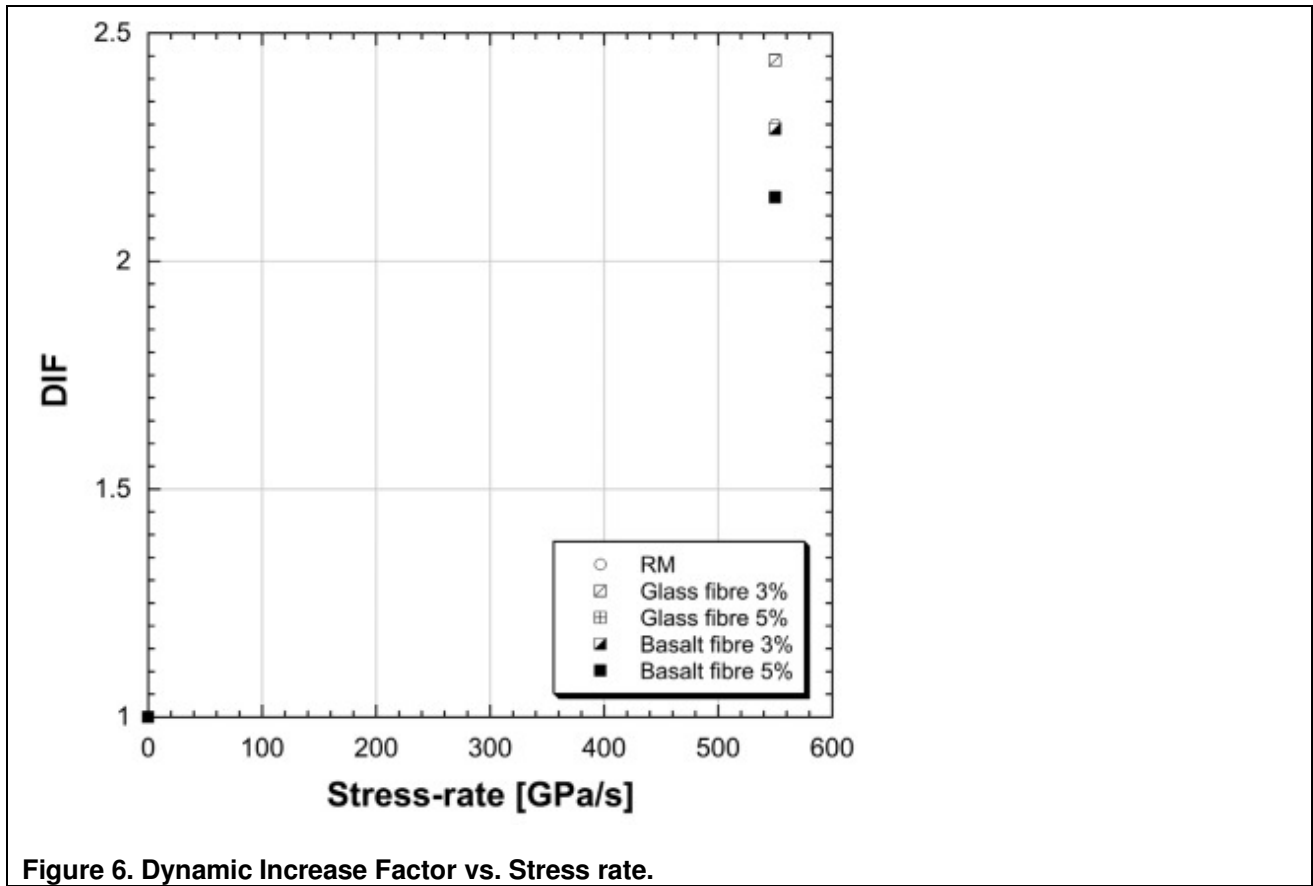


Figure 6. Dynamic Increase Factor vs. Stress rate.